High-Brightness Photocathodes through Ultrathin Surface Layers on Metals

Károly Németh,[1,2,*] Katherine C. Harkay,[1] Michel van Veenendaal,[1,2] Linda Spentzouris,[1,3] Marion White,[1] Klaus Attenkofer,[1] and George Srajer[1]

[1]*Advanced Photon Source, Argonne National Laboratory, Argonne, Illinois 60439, USA*
[2]*Department of Physics, Northern Illinois University, DeKalb, Illinois 60115, USA*
[3]*Illinois Institute of Technology, Chicago, Illinois 60616, USA*
(Received 22 September 2009; published 26 January 2010)

We report how ultrathin MgO films on Ag(001) surfaces can be used to control the emittance properties of photocathodes. In addition to substantially reducing the work function of the metal surface, the MgO layers also favorably influence the shape of the surface bands resulting in the generation of high-brightness electron beams. As the number of MgO surface layers varies from 0 to 3, the emitted electron beam becomes gradually brighter, reducing its transverse emittance to 0.06 mm mrad. We suggest the use of such photocathodes for the development of free-electron x-ray lasers and energy-recovery linac x-ray sources.

DOI: 10.1103/PhysRevLett.104.046801 PACS numbers: 73.20.At, 73.21.Ac, 73.21.Fg

High-brightness electron sources are critical prerequisites for the development of future x-ray energy-recovery linacs (XERL) and free-electron lasers (XFEL). State-of-the-art FEL electron injectors provide electron bunches of about 1 nC charge with 1 mm mrad emittance normalized to the beam energy and operate with a repetition rate of 120 Hz or less [1,2]. The goal for future high coherence XERLs [3] and XFEL oscillators [4] is about 0.1 mm mrad normalized emittance with lower bunch charge but with repetition rates of 1 MHz or more. High-brightness electron sources are, therefore, a rapidly evolving area of research and development. The majority of the effort is on electron sources using conventional photocathode materials, such as metals or semiconductors. Other alternatives include plasma-based sources [5,6] and photofield emitters [7]. Even in the case of large electron-bunch charge and perfect emittance compensation, the fundamental cathode emittance is an important contribution to the ultimate beam brightness [8]. According to recent work, the maximum achievable brightness depends only on the applied electric field to the cathode and the intrinsic emittance and is independent of the bunch charge [9]. The intrinsic emittance depends on many factors, e.g., the emitted momentum distribution, the surface roughness, nonuniformity, and impurities (e.g., oxide layers), grain boundaries, and the laser energy and polarization. The challenge is to combine all of the relevant phenomena into a complete and useful physical model.

In order to find a way to systematically tune the emittance properties of photocathodes, we have investigated systems in the distant field of surface catalysis. Ultrathin oxide layers on metal surfaces are known as a means to tune and control the catalytic activity of deposited metal clusters [10,11] through the thickness of the oxide layer. These systems are well known for the reduction of the work function compared to pure metals and for the charging of deposited clusters due to electrons tunneling through the oxide layers. Reduction of the work function of metals is potentially advantageous for photocathode development as it allows for the use of relative low-energy lasers with a typical photon energy of $\varepsilon_{\rm ph} = 4.66$ eV, while work functions of transition metals (Cu, Ag, Au, etc.) are approximately in the 4–5 eV range. The tunability of electron transfer through oxide layer thickness is also attractive, as it suggests that the shape of the surface bands responsible for the emittance can be controlled by the same means. The normalized intrinsic emittance of a photocathode can be defined [12] as $\varepsilon_{n,\rm int} = \beta\sigma_x\sigma_{x'}$, where $\beta = v/c$, with v being the mean velocity of the emitted electrons, σ_x is the laser illumination radius on the photocathode, and $\sigma_{x'} = \arcsin(\sigma_{p_x}/p)$, with σ_{p_x} being the spread (root mean square deviation) of the surface-parallel momentum and p the mean total momentum of the emitted electrons. In a typical situation, $\sigma_x = 0.3$ mm. Since the surface-parallel crystal momentum of the electrons is preserved upon emission from excited states [13], and supposing that the excited states are generated through direct (k-preserving) transitions, the spread of the surface-parallel momentum can be given as $\sigma_{p_x} = \hbar k_{\rm max}$, with $k_{\rm max}$ being the radius of the occupied region of the surface band in reciprocal space, if only one surface band contributes to the emission. Thus, our goal here is to limit the emission to a single surface band and to make $k_{\rm max}$ as small as possible through varying the number of surface oxide layers.

A frequently investigated system with tunable properties is the (001) surface of Ag or Mo with typically 2–3 monolayers (ML) of MgO, as shown in Fig. 1. The charging of gold atoms and clusters has been studied on these surfaces [14–20]. Both Ag and MgO form a fcc lattice with nearly identical lattice constants (4.216 and 4.086 Å, for MgO and Ag, respectively), which helps the formation of well-matching interfaces. The gold atoms and clusters are negatively charged in these systems due to transfer of electrons

 © 2010 The American Physical Society

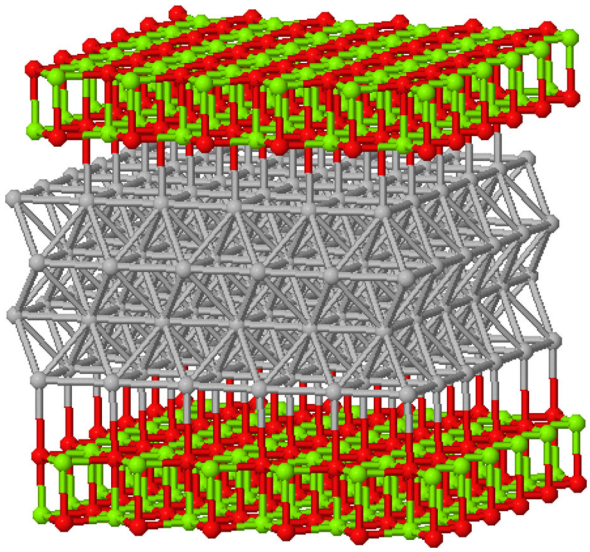

FIG. 1 (color online). The structure of the model system for 2 ML MgO(001) on the upper and lower surfaces of 4 ML Ag(001), denoted here as MgO(2 ML)/Ag(001)(4 ML)/MgO(2 ML). Interface Ag atoms (gray, center) are only attached to O atoms (red), and not to Mg (green).

from the Ag (or Mo) substrate through the ultrathin MgO layer. The charge transfer is a consequence of a substantial 1–2 eV work function reduction of the metal substrate induced by the addition of the ultrathin MgO layer [21,22]. Though the size of the work function reduction can be estimated well with the Schottky model [23] for the MgO/Ag(001) system, its interpretation is more complex in general [21]. Gold atoms and clusters can also be positively charged, e.g., on FeO/Pt(111) surfaces [24]. Not only the ultrathin layers of MgO over Ag(001) have been studied, but also those of Ag over MgO(001) [25–27]. It has been pointed out that the binding energy of Ag over MgO(001) is a damped oscillatory function of the number of monolayers that saturates at about 4 ML. Similar oscillatory changes can be observed in the band structure [25]. During epitaxial growth, up to 4–6 ML, Ag typically forms islands of ~9 nm width that perfectly fit to MgO(001), further epitaxial growth typically results in mismatch of the two lattices [27]. A thorough review of electronic excitations at metal surfaces can be found in Ref. [28].

In this Letter, we demonstrate that the surface electronic structure can be tailored by varying the number of oxide layers, and this has a strong manifestation in the brightness of emitted electrons. Our model system consists of a 4 ML Ag(001) slab covered by n_{MgO} MLs of MgO on both the top and bottom [denoted as MgO(n_{MgO}ML)/Ag(001)(4 ML)/MgO(n_{MgO}ML); see Fig. 1]. Thin Ag(001) slabs also have the advantage that their bands show increased sensitivity to MgO deposition as compared to thicker ones. We have carried out band-structure calculations using the PWSCF code [29] with norm-conserving pseudopotentials [30] and the PW91 density functional [31] with a wave-function cutoff of 100 Ry and a k-space grid of $8 \times 8 \times 8$ points for bulks and $8 \times 8 \times 1$ for surface slabs. Periodic boundary conditions were set for all lattice directions, and a vacuum layer of at least 15 Å was used to separate surface slabs. Work functions were determined similarly to Ref. [32]. The pseudopotentials reproduce experimental lattice constants of MgO and Ag with less than 2% error, bulk moduli within 6% for Ag (calculated value 94, experimental 100 GPa) and within 9% for MgO (calculated 145, experimental 160 GPa), the Ag-O distance in Ag(1 ML)/MgO(001)(4 ML) within 5%–8% (experimental 2.52 ± 0.1 Å, [27]). The calculated work function of 4 ML Ag(001) is 4.25 eV (experimental

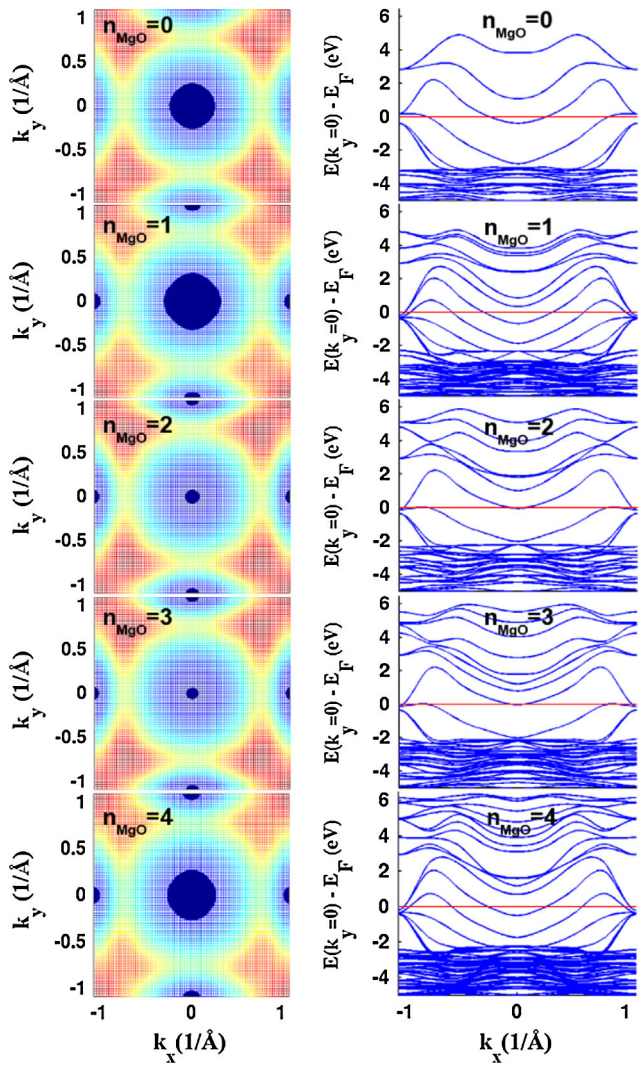

FIG. 2 (color online). Surface bands (left-hand panels) and the band structure (right-hand panels) of MgO(n_{MgO}ML)/Ag(001)(4 ML)/MgO(n_{MgO}ML) systems in the Brillouin zone for $n_{\mathrm{MgO}} = 0$–4. Dark blue spots denote k-space regions with occupied electrons; otherwise, coloring indicates band height above E_F, the Fermi energy. Only surface bands with the highest energy occupied crystal orbitals in the center of the Brillouin zone are shown for each value of n_{MgO}.

4.64 eV), that of MgO(2 ML)/Ag(001)(4 ML)/MgO(2 ML) is 3.08 eV (3.10 eV in Ref. [21]). All our calculations have also been checked with ultrasoft pseudopotentials with both PW91 and PBE [33] density functionals as available with PWSCF, producing very similar results. Here we present only data obtained from calculations with norm-conserving pseudopotentials. The methodology presented here has been used in numerous surface studies (see those mentioned above) with similar accuracy. The correspondence between the calculated $k_{\max}$ and the angle distribution of photoelectrons has been pointed out [e.g., in Ref. [34] for Cu(001)]; our calculations confirm the same $k_{\max}$ value and those calculated for several other surfaces [35]. The two surface lattice vectors are perpendicular, lay along the x and y axes, and are fixed at 2.889 Å corresponding to the (001)-cleaved experimental Ag crystal structure. All atomic positions were relaxed until the maximum Cartesian force component decreased to less than 0.0001 Ry/bohr. All properties presented are from the relaxed geometries.

Since surface slabs have only 2D periodicity, one can visualize the electronic bands as 3D surfaces as shown in Fig. 2. It is remarkable that one can see a clear tendency in the radius of the occupied region ($k_{\max}$) in the center of the Brillouin zone (at the Γ point, where $k_x = k_y = 0$), as a function of n_{MgO}, with a minimum at $n_{\mathrm{MgO}} = 2, 3$. This tendency has been observed only with a thin enough ($\ll$8 ML) Ag layer and only if MgO covered both sides of the Ag layer. The MgO layers impose vertical boundary conditions on the electronic states of the thin Ag layer and act as a perturbing potential. Because of these effects the surface bands of the Ag layer can sensitively be tuned by varying the number of MgO layers. To achieve significant sensitivity, both a thin Ag layer and top and bottom MgO overlayers are required. The calculated work functions are all close to 3 eV: 3.34 eV for $n_{\mathrm{MgO}} = 1$, 3.08 eV for $n_{\mathrm{MgO}} = 2$, and 3.11 eV for $n_{\mathrm{MgO}} = 3$. In our case with the given laser parameters, for the $n_{\mathrm{MgO}} = 2, 3$ systems only the highest energy occupied surface states at the Γ point will contribute to the emission, since the next occupied level is $\approx$2 eV below E_F, the Fermi energy, and the 4.66 eV photon energy is not sufficient to excite electrons from this level to levels above the vacuum potential, $E_{\mathrm{vac}} = E_F + \Phi$, with Φ being the work function, and $\Phi \approx$ 3 eV. Emission from k points far from the Γ point is not possible for a similar reason, since for such emission $(\hbar k)^2/2m_e$ extra photon energy would be needed [13], with m_e the electron's rest mass. The highest energy surface states at the Γ point are dominated by the $5p_z$ states of the topmost Ag atoms with some contribution of the $5s$ of the same atoms and the $2p_z$ states of the directly attached O atoms. The unoccupied states 4.02 and 5.11 eV above these occupied ones are dominated by the $3s/p_z$ and the $2s$ states of the outermost Mg and O atoms, respectively. Excitation to these levels brings electrons directly to the outer surface of the MgO layers where they can be emitted without any further travel through the MgO layers. Assuming that unoccupied states exist for photoexcitation, one obtains $\varepsilon_{n,\mathrm{int}} = 0.06$ mm mrad ($k_{\max} = 0.05$ 1/Å) for the intrinsic emittance, which is less than the desired 0.1 mm mrad for the applications mentioned above. However, this assumption is actually a poor one for a single MgO/Ag(001) $\times$ (4 ML) system, as the excitation energies do not exactly coincide with the typical photon energy of 4.66 eV. One way to improve the probability of absorbing such a photon is to build an alternating vertical stack of 4 ML Ag(001) and n_{MgO} ML MgO layers. For example, in an alternating stack containing three isolated 4 ML Ag(001) layers, i.e., $[\mathrm{MgO(2\ ML)/Ag(001)(4\ ML)/}]_3/\mathrm{MgO(2\ ML)}$, the surface bands of a single 4 ML Ag(001) layer will be split in three as a consequence of the interaction of three 4 ML Ag(001) layers, while $k_{\max}$ of the highest energy occupied surface states is preserved and the excitation energy at the Γ point becomes 4.71 eV, close to the photon energy.

In practice, ultrathin MgO layers on Ag(001) form terraces of typically 50 nm width [14], due to surface roughness, and the typical surface density of point defects within the terraces is $<$0.1% per ML [36]. While this level of defect density is most likely acceptable as it preserves the homogeneity of the model for large surface areas within a single Ag/MgO interface, for multiple overlayered structures it may lead to deviation from the ideal predicted beam brightness. One way to improve surface homogeneity could be based on a construct depicted in Fig. 3. In this construct, Ag nanorods [37,38] of 50–200 nm width and several μm length are embedded into a MgO matrix along the (001) faces. The embedding may take place by repeated 50–200 nm wide Ag depositions followed by etching 50–200 nm wide gaps into the Ag layer, filling the gap with MgO, and building an insulating MgO layer, again of 50–200 nm width. The repeated process would terminate when the width of the embedded system equals the laser illumination diameter (typically $2\sigma_x = 0.6$ mm). The resulting final embedded system of nanorods would form a

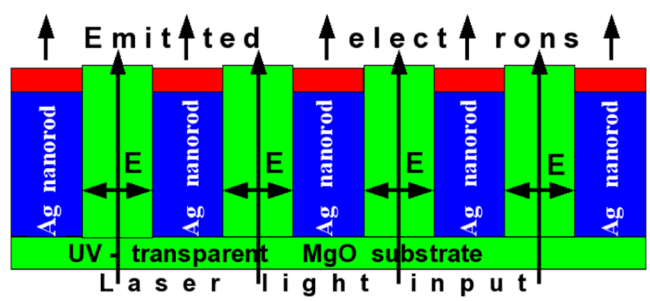

FIG. 3 (color online). Schematic of a photocathode based on a multilayer (red rectangle) topped Ag-nanorod array embedded in a UV-transparent MgO substrate. Typical dimensions of the nanorods are 50–200 nm width and several μm length; the space between the nanorods is commensurate with the width of the nanorods.

$2\sigma_x \times 2\sigma_x$ base-sized prism in MgO matrix. The surface of the embedded system perpendicular to the nanorods is polished. Then the nanorods would be etched back through the open Ag terminations leaving a hole into which multilayers can be deposited. Before each layer is deposited, the surface over the nanorods may be annealed by laser illumination in order to produce as defectless a surface as possible. The laser light will selectively heat the area above the nanorods, as it is not absorbed by MgO. The preferred way of depositing the Ag layers could be based on electrochemistry, since only the space above the nanorods would be a conductive area. When MgO is deposited, e.g., reactive sputtering (as usual) could be used. It is expected that this way selective deposition into the holes could happen with repeated annealing and minimizing the occurrence of defects. The first MgO layers deposited on top of the nanorods can be as wide as 8–10 ML [16] allowing for electron tunneling but not for emission from the nanorods into vacuum. A further advantage of the proposed realization of the Ag/MgO photocathode is that the E field of the laser can be perpendicular to an Ag/MgO interface in reflection or transmission mode, at illuminations from front or back or at grazing incidence. Grazing incidence typically improves the absorption probability of the photon by 1–2 orders of magnitude [39] and greatly increases the quantum yield of the photocathode. Transmission mode also protects the multilayers from possible damage through direct illumination. The quantum yield is typically calculated through semiempirical formulas using experimentally determined reflectivity and attenuation length of light [40–43], which cannot be applied here, as the system has not been realized yet. This Letter intends to focus only on the fundamental aspect of controlling the transverse emittance through oxide overlayers.

In conclusion, we have pointed out that ultrathin oxide layers on metal surfaces provide a means to control the transverse emittance of photoemitted electron beams. The transverse emittance (brightness) of the beam is a function of the number of oxide layers. We have also described a photocathode design that makes use of this approach of emittance control. Further computational screening of other metal-oxide systems with potential for high-brightness photocathodes will be continued, along with related emittance measurements.

The authors thank NERSC (U.S. DOE DE-AC02-05CH11231) for the use of computational resources. This research was supported by the U.S. DOE Office of Science, under Contracts No. DE-AC02-06CH11357 and No. DE-FG02-03ER46097.

*Nemeth@ANL.Gov

[1] R. Akre *et al.*, Phys. Rev. ST Accel. Beams **11**, 030703 (2008).
[2] K. Togawa *et al.*, Phys. Rev. ST Accel. Beams **10**, 020703 (2007).
[3] I. V. Bazarov *et al.*, in *Proceedings of the 2001 Particle Accelerator Conference, Chicago* (IEEE, New York, 2001), p. 230.
[4] K.-J. Kim *et al.*, Phys. Rev. Lett. **100**, 244802 (2008).
[5] B. J. Claessens *et al.*, Phys. Rev. Lett. **95**, 164801 (2005).
[6] M. Zolotorev *et al.*, Phys. Rev. Lett. **98**, 184801 (2007).
[7] R. Ganter *et al.*, Phys. Rev. Lett. **100**, 064801 (2008).
[8] I. V. Basarov *et al.*, Phys. Rev. ST Accel. Beams **8**, 034202 (2005).
[9] I. V. Basarov *et al.*, Phys. Rev. Lett. **102**, 104801 (2009).
[10] H.-J. Freund *et al.*, Chem. Soc. Rev. **37**, 2224 (2008).
[11] H.-J. Freund, Surf. Sci. **601**, 1438 (2007).
[12] J. Lawson, *The Physics of Charged-Particle Beams* (Clarendon Press, Oxford, 1988).
[13] M. Cardona and L. Ley, in *Photoemission in Solids I. General Principles*, edited by L. Ley and M. Cardona, Topics in Applied Physics Vol. 26 (Springer, Berlin, 1978), Chap. 1.6, p. 84.
[14] S. Schintke *et al.*, Phys. Rev. Lett. **87**, 276801 (2001).
[15] G. Pacchioni *et al.*, Phys. Rev. Lett. **94**, 226104 (2005).
[16] M. Sterrer *et al.*, Phys. Rev. Lett. **98**, 206103 (2007).
[17] X. Lin *et al.*, Phys. Rev. Lett. **102**, 206801 (2009).
[18] L. Giordano *et al.*, Phys. Chem. Chem. Phys. **8**, 3335 (2006).
[19] L. Giordano *et al.*, J. Chem. Phys. **127**, 144713 (2007).
[20] V. Simic-Milosevic *et al.*, Phys. Rev. B **78**, 235429 (2008).
[21] L. Giordano *et al.*, Phys. Rev. B **73**, 045414 (2006).
[22] T. König *et al.*, J. Phys. Chem. C **113**, 11 301 (2009).
[23] W. Schottky, Phys. Z. **41**, 570 (1940).
[24] L. Giordano *et al.*, Phys. Rev. Lett. **101**, 026102 (2008).
[25] J.-H. Cho *et al.*, Phys. Rev. B **63**, 113408 (2001).
[26] A. M. Flank *et al.*, Phys. Rev. B **53**, R1737 (1996).
[27] O. Robach *et al.*, Phys. Rev. B **60**, 5858 (1999).
[28] E. V. Chulkov *et al.*, Chem. Rev. **106**, 4160 (2006).
[29] P. Gianozzi *et al.*, J. Phys. Condens. Matter **21**, 395502 (2009); http://www.quantum-espresso.org.
[30] A. M. Rappe *et al.*, Phys. Rev. B **41**, 1227 (1990).
[31] J. P. Perdew *et al.*, Phys. Rev. B **46**, 6671 (1992).
[32] Y. Ikuno *et al.*, e-J. Surf. Sci. Nanotechnology **6**, 103 (2008).
[33] J. P. Perdew, K. Burke, and M. Ernzerhof, Phys. Rev. Lett. **77**, 3865 (1996).
[34] S. D. Kevan, Phys. Rev. B **28**, 2268 (1983).
[35] K. C. Harkay *et al.*, in Proceedings of the 2009 Particle Accelerator Conference, Vancouver (IEEE, New York, to be published).
[36] U. Heiz *et al.*, J. Phys. D **33**, R85 (2000).
[37] S. Guo *et al.*, Cryst. Growth Des. **9**, 372 (2009).
[38] P. L. Taberna *et al.*, Nature Mater. **5**, 567 (2006).
[39] D. Xiang *et al.*, Nucl. Instrum. Methods Phys. Res., Sect. A **562**, 48 (2006).
[40] C. N. Berglund and W. E. Spicer, Phys. Rev. **136**, A1030 (1964); **136**, A1044 (1964);
[41] K. L. Jensen *et al.*, J. Appl. Phys. **99**, 124905 (2006).
[42] E. Pedersoli *et al.*, Appl. Phys. Lett. **93**, 183505 (2008).
[43] D. H. Dowell *et al.*, Phys. Rev. ST Accel. Beams **12**, 074201 (2009).